Superconductivity in noncentrosymmetric ternary equiatomic pnictides La*MP* (*M* = Ir and Rh; *P* = P and As)

Yanpeng Qi,[1] Jiangang Guo,[1] Hechang Lei,[1] Zewen Xiao,[2] Toshio Kamiya,[2] and Hideo Hosono[1,2,*]
[1]*Frontier Research Center, Tokyo Institute of Technology, 4259 Nagatsuta, Midori, Yokohama 226-8503, Japan*
[2]*Materials and Structures Laboratory, Tokyo Institute of Technology, 4259 Nagatsuta, Midori, Yokohama 226-8503, Japan*
(Received 18 November 2013; revised manuscript received 7 January 2014; published 31 January 2014)

We report bulk superconductivity of ternary equiatomic pnictides La*MP* (*M* = Ir and Rh; *P* = P and As) along with the crystal structure and physical properties (resistivity, magnetization, and heat capacity). It crystallized in a noncentrosymmetric structure type (space group $I4_1md$, $Z = 4$), which is an ordered ternary derivative of the centrosymmetric α-$ThSi_2$ structure. Three ternary pnictides showed superconductivity at low temperatures, and the highest critical temperature, $T_c = 5.3$ K, was observed for LaIrP. The experimental and density functional calculations results suggested that La*MP* could be categorized as a Bardeen–Cooper–Schrieffer superconductor with intermediate coupling. Considering the similar Sommerfeld value and Debye temperature, the differences in T_c were attributed to the difference in the electron-phonon coupling strength in the compounds.

DOI: 10.1103/PhysRevB.89.024517 PACS number(s): 74.70.Xa, 74.25.N−

I. INTRODUCTION

Since the discovery of superconductivity in the heavy element noncentrosymmetric compounds $CePt_3Si$ [1] and Li_2Pd_3B [2], superconductivity in systems lacking spatial inversion symmetry has attracted widespread research interest. The absence of inversion symmetry raises the possibility of antisymmetric spin-orbit coupling (ASOC), which can lift the degeneracy of the conduction band electrons and may lead to the formation of Cooper pairs of noncentrosymmetric superconductors due to the admixing of spin-singlet with spin-triplet states. It may also lead to various exotic electromagnetic properties, such as a high upper critical field far beyond the Pauli-Clogston limit, line nodes in the superconductivity gap function, or the involvement of spin-triplet pairs in the superconductivity condensate [3–6].

The discovery of high T_c superconductivity in iron pnictides has rekindled extensive exploration of new superconductors in metal pnictides [7]. Among them, the ternary equiatomic pnictides with the general formula $M'MP$ (where M' is a large-sized, electropositive transition metal from the left side of the periodic table, M is a small transition metal, and P is a pnictogen) compose a large compound family showing interesting physical properties at low temperatures. Indeed, superconductivity has previously been reported in those compounds with hexagonal structure or orthorhombic structure [8,9]. Although ternary equiatomic $M'MP$ compounds have already been widely studied, the transition metal M has generally been a 3*d* metal. Hence, it is of interest to synthesize new ternary equiatomic compounds with a higher *d* orbital (4*d* or 5*d*) and to examine their physical properties at low temperatures.

In this paper, we report the synthesis of ternary equiatomic pnictides La*MP* (*M* = Ir and Rh; *P* = P and As) using high-pressure technology, finding bulk superconductivity with transition temperatures 5.3 K, 3.1 K, and 2.5 K for LaIrP, LaIrAs, and LaRhP, respectively. La*MP* crystallized in its own noncentrosymmetric structure (tetragonal, space group $I4_1md$, $Z = 4$). This is the first superconducting report in ternary equiatomic pnictides with the LaPtSi-type structure. The characterization implies that ASOC is not strong enough to induce unconventional superconducting properties in La*MP* compounds. Considering the similar Sommerfeld values and Debye temperatures, the variation in superconducting transition temperatures is attributed to the differences in magnitude of electron-phonon coupling strength in the compounds.

II. EXPERIMENTAL AND COMPUTATIONAL DETAILS

Polycrystalline samples of La*MP* (*M* = Ir and Rh; *P* = P and As) were synthesized by solid state reactions under high pressure. First, the LaP and LaAs were prepared from respective elements in an evacuated silica tube. High-purity powders of Ir or Rh were mixed with LaP or LaAs at the desired ratio and were placed in an *h*-BN capsule and then heated at 1673 K and 5 GPa for 2 h using a belt-type high-pressure apparatus. All starting materials and precursors for the synthesis were prepared in a glove box filled with purified Ar gas (H_2O, $O_2 < 1$ ppm).

The phase identification of the resulting samples was carried out by powder x-ray diffraction (PXRD) using a Bruker diffractometer (model D8 ADVANCE; Cu rotating anode). Rietveld refinement of the PXRD patterns was performed using the TOPAS code [10]. Elemental compositions were determined using an electron-probe microanalyzer (EPMA, JEOL, Inc., model JXA-8530F). The dependence of dc electrical resistivity was measured by the conventional four-probe method with a physical property measurement system (PPMS, Quantum Design). Magnetic measurements were performed using a vibrating sample magnetometer (Quantum Design). Specific heat data were obtained with the PPMS using the conventional thermal relaxation method.

Density functional theory (DFT) calculations were performed using the projected augmented plane-wave method implemented in Vienna *Ab initio* Simulation Package 5.3.3 code [11]. The Perdew-Burke-Ernzerhof [12] general gradient approximation was used for the exchange-correlation potential. The lattice parameters and atomic positions were fully

*Corresponding author: hosono@msl.titech.ac.jp

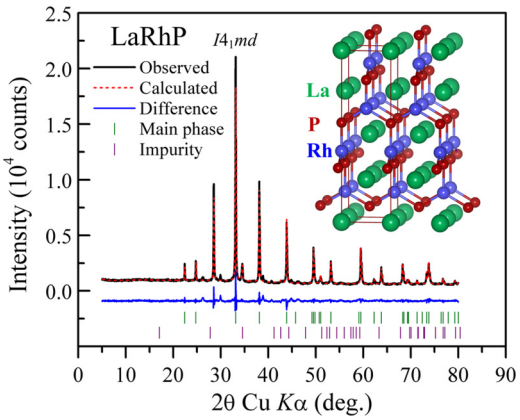

FIG. 1. (Color online) PXRD pattern of LaRhP representing La*MP* compounds. The inset shows the crystal structure of LaRhP.

relaxed by a structural optimization procedure minimizing the total energy and force. Self-consistent solutions of the Kohn-Sham equations were obtained by employing a $7 \times 7 \times 2$ Monkhorst-Pack grid of k-points for integration over the Brillouin zone, and the plane-wave basis-set cutoff was set to 583.6 eV. The full electronic density of states (DOS) was also calculated with a high k-point sampling of $14 \times 14 \times 4$.

III. RESULTS AND DISCUSSION

Figure 1 shows the XRD pattern of the LaRhP sample, representing La*MP* (M = Ir and Rh; P = P and As) compounds. Except for the peaks arising from the slight RhP_3 impurity, all peaks could be attributed to the tetragonal structure (space group $I4_1md$, $Z = 4$) with $a = 4.1275$ Å and $c = 14.3839$ Å. The corresponding crystallographic data are summarized in Table I. From the quality of the XRD data, the Rietveld refinement estimated the purity of LaRhP as ~95%. In the subsequent magnetic measurements, it was shown that the superconducting component exceeded 90%, confirming the superconductivity in the title compounds originating from the main phase. The fitted lattice parameters of the other three compounds are also listed in Table I. The lattice parameters of LaRhAs and LaIrP obtained in this work are in good agreement with data reported previously in Refs. [13] and [14]. The inset in Fig. 1 shows the crystal structure of LaRhP, which is an ordered ternary derivative structure of the α-$ThSi_2$ type [15]. The Rh and P atoms are linked to form a three-dimensional network with a trigonal planar environment, whereas the La atoms are located in the cavities. The Rh-P framework comprised two sets of perpendicular Rh-P zig-zig chains. The Rh-P separation in the intrachain is close to that in the interchain; the Rh-P bond angles are also almost identical, with only a slight deviation from 120°. As for the space group $I4_1md$, which belongs to the point group $4mm$, the crystal structure has no inversion symmetry. For example, the Rh atom's sublattice does not possess an inversion system along the c axis; thus, the inversion symmetry is broken along this direction. The chemical composition analysis by EPMA demonstrated the one-to-one correspondence between actual and nominal compositions.

Figure 2(a) shows the temperature dependence of the electrical resistivity for the La*MP* (M = Ir and Rh; P = P and As) compounds in the temperature range 1.9–300 K. All samples exhibited metallic behaviors in the whole temperature range. At low temperatures, a sharp drop in $\rho(T)$ to zero was observed, suggesting the onset of a superconducting transition. The inset of Fig. 2(a) shows an enlargement of the superconducting transition. The transition temperatures T_c were 5.3 K, 3.1 K, and 2.5 K for LaIrP, LaIrAs, and LaRhP, respectively. The transition widths ΔT_c were all approximately 0.2 K, implying fairly good sample quality. For the LaRhAs, however, the $\rho(T)$ curve still showed normal metal behavior; no superconducting transition was observed down to the lowest measuring temperature.

In the normal state (5 K $< T <$ 25 K), the temperature dependence of $\rho(T)$ could be fitted to a power-law relation,

$$\rho = \rho_0 + aT^n, \tag{1}$$

which yields an optimum value of 3 for n. This value of n agrees with Wilson's s-d scattering model, which predicts a T^3 dependence of $\rho_1(T)$ for $T < \Theta_D/10$ [16]. At high temperature (40 K $< T <$ 300 K), the $\rho(T)$ data significantly deviate from linear temperature dependence, similar to that of LaPtSi compounds [17,18]. One of the models that describes the $\rho(T)$ of these compounds is known as the parallel resistor model [18,19]. In this model the expression of $\rho(T)$ is given by

$$\frac{1}{\rho(T)} = \frac{1}{\rho_1(T)} + \frac{1}{\rho_{\max}}, \tag{2}$$

TABLE I. Structural parameters and Wyckoff positions of La*MP* (M = Ir and Rh; P = P and As).

Compound	LaRhP	LaRhAs	LaIrP	LaIrAs
Space group(Z)		$I4_1md$ or No. 109 ($Z = 4$)		
Crystal structure		Ternary derivative of α-$ThSi_2$		
Lattice parameter: a	4.1846 Å	4.1257 Å	4.2065 Å	4.1505 Å
Lattice parameter: c	14.9358 Å	14.3839 Å	14.9379 Å	14.3277 Å
La on 4a z	0.0	0.0	0.0	0.0
M on 4a z	0.4215	0.4143	0.4197	0.4126
P on 4a z	0.5857	0.5815	0.5839	0.5754
Rh/Ir-P distance	2.3827 Å	2.4520 Å	2.3789 Å	2.4533 Å
	2.4051 Å	2.4538 Å	2.3993 Å	2.4628 Å
P-Rh/Ir-P angle	119.98°	117.01°	119.25°	117.30°
	120.03°	121.49°	120.77°	121.35°

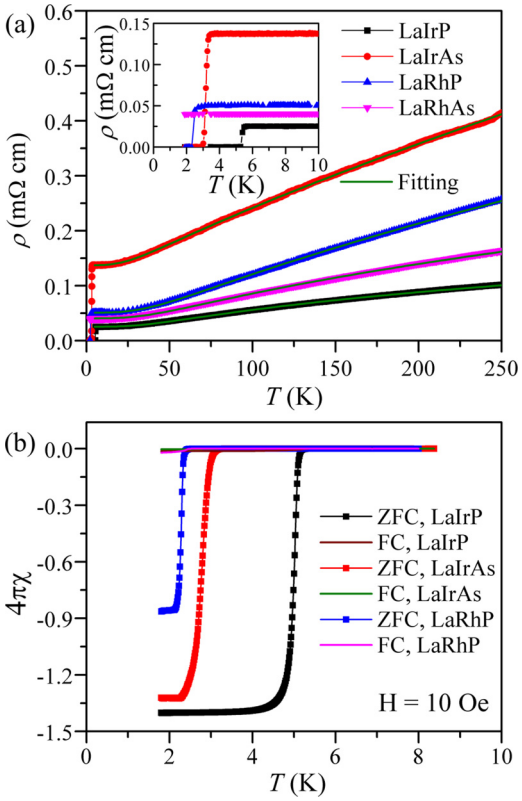

FIG. 2. (Color online) Temperature dependence of resistivity and magnetism. (a) Resistivity $\rho(T)$ of LaMP (M = Ir and Rh; P = P and As). The solid lines show the fits (see text). Inset: Enlarged view of the low-temperature region, showing the superconducting transition. (b) Dc-magnetization data at low temperatures under an applied magnetic field of 10 Oe. Large diamagnetic signals were clearly observed below T_c, indicating bulk superconductivity in the samples.

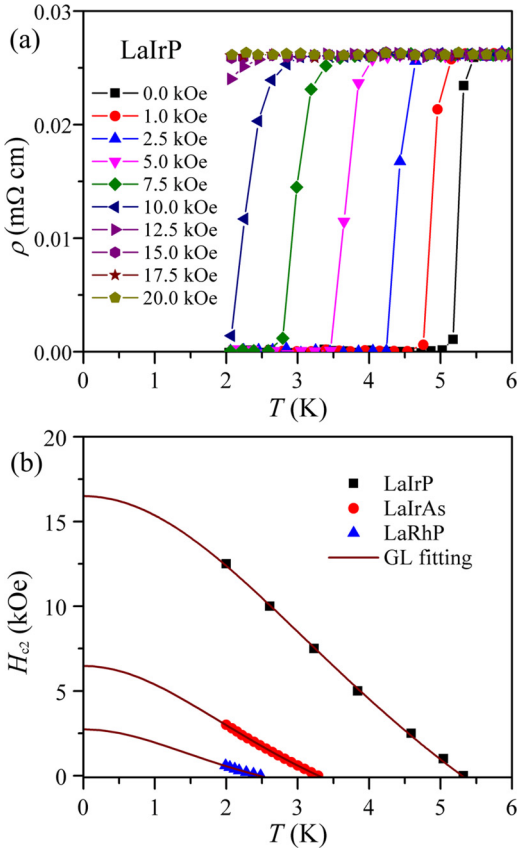

FIG. 3. (Color online) Effects of magnetic field on superconducting properties. (a) Temperature dependence of resistivity measured at various magnetic fields for LaIrP. (b) Temperature dependence of H_{c2} of LaMP (M = Ir and Rh; P = P and As). The solid line shows the fitting result using the Ginzburg-Landau (GL) formula.

where $\rho_{\max}$ is the saturation resistivity, which is independent of temperature, and $\rho_1(T)$ is given by the following expression:

$$\rho_1(T) = \rho_0 + C_1\left(\frac{T}{\Theta_D}\right)^3 \times \int_0^{\Theta_D/T} \frac{x_3 dx}{[1-\exp(-x)][\exp(x)-1]}, \quad (3)$$

where ρ_0 is the residual resistivity and the second term is due to phonon-assisted electron scattering similar to the s-d scattering in transition metal alloys. Θ_D is the Debye temperature, and C_1 is a numerical constant. The resistivity data fitted to the above equations in the range 40–300 K yielded $\Theta_D = 294$ K, 240 K, 302 K, and 237 K for LaIrP, LaIrAs, LaRhP, and LaRhAs, respectively. As discussed below, these values are close to the ones measured by low temperature heat capacity.

Low temperature magnetization measurements on LaMP compounds were carried out in zero-field-cooling and field-cooling modes under 10 Oe in the low temperature region. As shown in Fig. 2(b), the rapid drop of the zero-field-cooling data denotes the onset of superconductivity, in fair agreement with resistivity results. The large diamagnetic signal at 1.8 K confirms the bulk superconductivity. The magnetization curves in the superconducting state show the typical behavior of type-II superconductors. The superconducting volume fractions at 1.8 K were larger than 100% for LaIrP and LaIrAs because of the uncorrected demagnetization factor of the samples.

Figure 3(a) shows the field broadening of the resistivity curves for the LaIrP compound with increasing magnetic fields. The superconducting transition gradually shifted to the lower temperature [20–22]. At $H = 20$ kOe, the superconducting transition could not be observed above 2 K. We plotted the upper critical field (H_{c2}) using the 90% points on the resistive transition curves as a function of temperature in Fig. 3(b). The value of the slope of H_{c2} for the LaIrP sample at T_c was 3.77 kOe/K. A simple estimate using the conventional one-band Werthamer–Helfand–Hohenberg (WHH) approximation without considering the Pauli spin paramagnetism effect and spin obit interaction [23], $H_{c2}(0) = -0.693 \times (dH_{c2}/dT) \times T_c$, yielded a value of ~13.8 kOe. We also tried to use the Ginzburg-Landau formula to fit the data determined by adopting the criterion of 90% $\rho_n(T)$,

$$H_{c2}(T) = H_{c2}(0)\frac{1-t^2}{1+t^2}, \quad (4)$$

where t is the normalized temperature T/T_c. It was found that the upper critical field $H_{c2} = 16.4$ kOe, which was slightly higher than that obtained using the WHH formula.

TABLE II. Parameters obtained for superconductivity of LaIrP, LaIrAs, and LaRhP.

Compound	LaIrP	LaIrAs	LaRhP
T_c/K	5.3	3.1	2.5
H_{c2} (WHH)/ kOe	13.8	5.5	2.1
H_{c2} (GL)/ kOe	16.4	6.4	2.7
$\xi_{GL}(0)$/nm	14.2	22.7	34.9
$\Delta C/\gamma T_c$	0.65	0.84	0.73
$\lambda_{\text{e-ph}}$	0.67	0.58	0.52

According to the relationship between H_{c2} and the coherence length ξ, namely, $H_{c2} = \Phi_0/(2\pi\xi^2)$, where $\Phi_0 = 2.07 \times 10^{-15}$ Wb is the flux quantum, the derived $\xi_{GL}(0)$ was 14.2 nm. The Pauli-Clogston limiting field $H_p(0) = 1.84T_c$ [24], yielding $H_p(0) = 97$ kOe for LaIrP, was obviously larger than the present value; therefore, the orbital effect should be the dominant pair-breaking mechanism in the LaIrP compound. This is the difference from the case of $CePt_3Si$ and Li_2Pt_3B [1,2] in which the high upper critical field is far beyond the Pauli-Clogston limit. Therefore, the ASOC induced by noncentrosymmetry should not be significant in LaIrP. Similar phenomena were observed in two other compounds, LaIrAs and LaRhP, and the corresponding data are summarized in Table II.

Further evidence for bulk superconductivity was obtained from the large specific-heat jumps at T_c, shown in Fig. 4(a). The temperatures corresponding to the distinct jump in C_p/T coincided with the electrical and magnetic data. The specific-heat curves in the low temperature range could be well fitted by $C_p/T = \gamma + \beta T^2 + \delta T^4$, implying that the influence of high-frequency acoustic phonon branches is more significant. The fitted curves yielded the Sommerfeld electronic coefficients γ = 9.07, 8.82, 6.96, and 7.71 mJ·mol^{-1}·K^{-2} for LaIrP, LaIrAs, LaRhP, and LaRhAs, respectively. The Debye temperatures calculated from the equation $\Theta_D = (12\pi^4 NR/5\beta)$ [1,3], where N is the number of atoms per formula unit and R is the gas constant, were 282 K, 261 K, 328 K, and 263 K for the respective four samples. It can be seen that the Debye temperatures Θ_D for these compounds are close to each other and also consistent with the values from resistivity analyses.

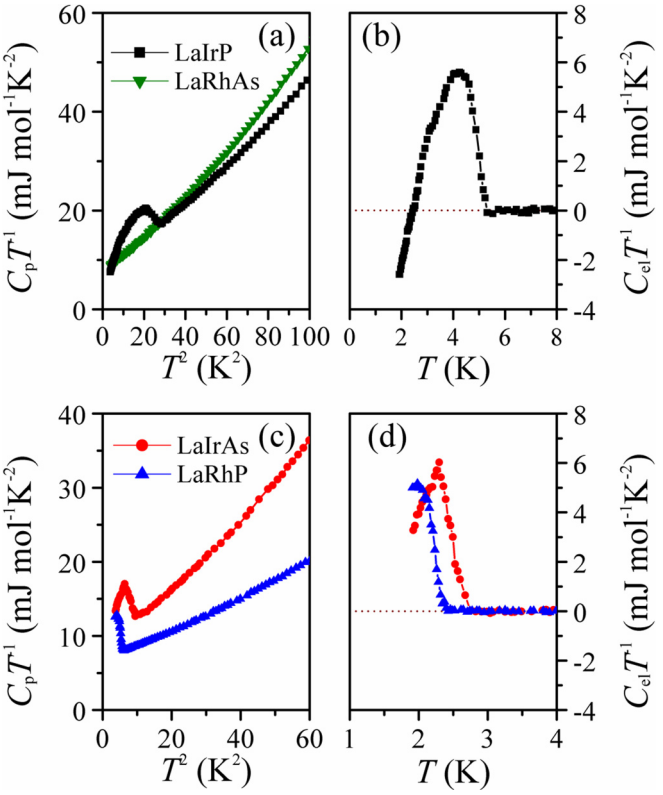

FIG. 4. (Color online) Low temperature heat capacity (C_p). (a), (c) C_p/T vs T^2 of LaMP (M = Ir and Rh; P = P and As). (b), (d) Temperature dependence of the electronic specific heat plotted as C_{el}/T vs T at zero field for superconducting compounds.

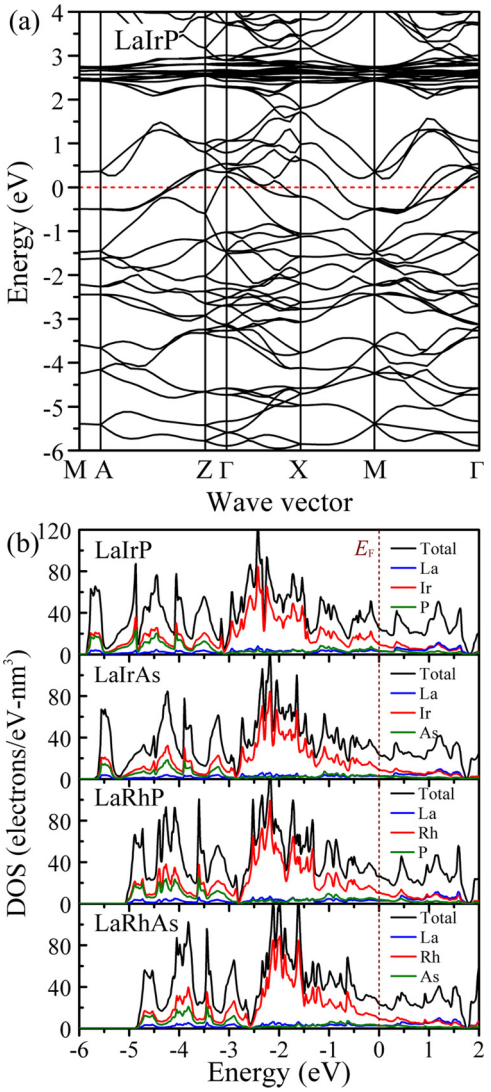

FIG. 5. (Color online) Calculated electronic structure. (a) Band structure of LaIrP. (b) The total and partial DOS curves for LaMP (M = Ir and Rh; P = P and As).

TABLE III. Debye temperature Θ_D derived from resistivity and heat capacity, normal-state electronic specific heat coefficient γ, derived $N(E_F)_T$ from γ, calculated $N(E_F)$, and calculated $N(E_F)_V$ of LaMP (M = Ir and Rh; P = P and As).

Compound	LaIrP	LaIrAs	LaRhP	LaRhAs
$\Theta_D(\rho(T))$/K	294	240	302	237
$\Theta_D(C_p)$/K	282	261	328	263
γ/mJ·mol^{-1}·K^{-2}	9.07	8.82	6.95	7.71
$N(E_F)_T$/states/eV f.u.	3.84	3.74	2.95	3.27
$N(E_F)$/states/eV f.u.	1.60	1.57	1.61	1.58
$N(E_F)_V$/states/eV nm^3	25.63	23.46	26.02	23.49

In addition, the γ is related to $N(E_F)$ by

$$\gamma = \frac{\pi^2}{3} k_B^2 N(E_F), \tag{5}$$

where k_B is the Boltzmann constant. The $N(E_F)$ was 3.84, 3.74, 2.95, and 3.27 states/eV f.u. for LaIrP, LaIrAs, LaRhP, and LaRhAs, respectively. These values are larger than the calculated values, as shown below, suggesting the presence of remarkable electron-phonon and/or electron-electron interaction. The electronic specific heat part C_{el} was obtained by subtracting the phonon contribution, as shown in Fig. 4(b). The normalized specific-heat jump values $\Delta C_{el}/\gamma T_c$ were estimated to be 0.65, 0.84, and 0.73 for LaIrP, LaIrAs, and LaRhP, respectively, which was substantially smaller than the Bardeen–Cooper–Schrieffer (BCS) weak-coupling limit value of 1.43 [25]. Small specific-heat jumps have also been observed in other superconductors and may be due to multiband effects or gap anisotropy [26,27].

Figure 5(a) shows the electronic band structure of LaIrP representing LaMP compounds. The band structures of the three other compounds were also calculated and are shown in Fig. 3S of the Supplemental Material [28]. In Fig. 5(b), we show the calculated total and partial DOS curves near E_F for the LaMP compounds. It should be noted that the units in which DOS were expressed were changed to states/eV nm^3 in order to compare the DOS values among these isostructural compounds. In the range -5 to -2 eV below the Fermi energy, the Ir or Rh band could be identified with some hybridization of the P or As orbital. At the Fermi energy, the transition metal (Ir or Rh) atoms are the main contributor to the DOS for all four compounds. Moreover, the $N(E_F)_{\rm cal}$ values (in units of states/eV f.u.) are listed in Table III and are very close to each other.

From Table III, we can see that the Debye temperatures and γ values for those compounds are close to each other, while the T_c values were obviously different. In addition, the $N(E_F)_{\rm cal}$ was much smaller than the derived values from specific heat measurements, suggesting that there are strong electron-phonon and/or electron-electron interactions. Next, we calculated the electron-phonon coupling constant $\lambda_{\text{e-ph}}$. According to the McMillan formula for electron-phonon mediated superconductivity [29], $\lambda_{\text{e-ph}}$ can be determined by

$$\lambda_{\text{e -ph}} = \frac{\mu^* \ln(1.45\, T_c/\Theta_D) - 1.04}{1.04 + \ln(1.45\, T_c/\Theta_D)(1 - 0.62\mu^*)}, \tag{6}$$

where $\mu = 0.13$ is the common value for Coulomb pseudopotential. By using our experimental values of T_c and Debye temperature, we obtained $\lambda_{\text{e-ph}} = 0.67$ for LaIrP, indicating an intermediately coupled superconductor. Moreover, the value for LaIrP was obviously larger than the $\lambda_{\text{e-ph}}$ values for LaIrAs and LaRhP: 0.58 and 0.52, respectively. Therefore, the higher T_c in LaIrP is attributed to the larger electron-phonon coupling constant $\lambda_{\text{e-ph}}$ when compared to the other two compounds.

A generally accepted description relies on the ASOC, which increases the spin degeneracy of the electronic bands. The effect of ASOC is a significant variant in different noncentrosymmetric superconductors. If the ASOC splitting is large, a genuine mixing of spin-singlet and spin-triplet components occurs. The strength of the ASOC is determined by the crystallographic structure and elemental composition. Although the crystal structure and unit cells of Li_2Pd_3B and Li_2Pd_3B are alike, their superconducting properties are distinctly different. The striking difference highlights the role of composition: increasing the ASOC by replacing Pd with Pt changes the superconducting order parameter from dominantly spin-singlet to nodal, spin-triplet. On the other hand, an upper critical field well below the standard paramagnetic limit and a BSC-like temperature-dependent heat capacity are observed in the noncentrosymmetric superconductor $Mg_{10}Ir_{19}B_{16}$ even with the heavy transition element Ir. This suggests that the crystal structure might be significant in $Mg_{10}Ir_{19}B_{16}$ compounds compared with the elemental composition. In the present ternary-pnictide noncentrosymmetric superconductors, BCS-type superconducting properties have been observed in both 4d-orbital compound LaRhP and 5d-orbital compound LaIrP. A possible explanation for the absence of unconventional superconducting properties is the lesser extent of noncentrosymmetry. The ASOC induced by noncentrosymmetry is not significant in the LaMP compounds.

IV. SUMMARY

We report on the synthesis, crystal structure, and physical properties (resistivity, magnetization, and heat capacity) in combination with DFT calculations for ternary equiatomic pnictides LaMP (M = Ir and Rh; P = P and As). Each LaMP crystallized into its own noncentrosymmetric-structure type (space group $I4_1$md, $Z = 4$), and superconductivity was found at $T_c = 5.3$ K, 3.1 K, and 2.5 K for LaIrP, LaIrAs, and LaRhP, respectively. The upper critical fields H_{c2} were not beyond the Pauli-Clogston limit, suggesting the ASOC induced by noncentrosymmetry is not significant in the LaMP compounds. The DFT calculations reveal that the transition metal Ir or Rh bands dominated the Fermi level in those compounds. Considering the similar Sommerfeld values and Debye temperatures, the differences in T_c in LaMP compounds were attributed to differences in electron-phonon coupling.

ACKNOWLEDGMENTS

This work was supported by the Funding Program for World-Leading Innovative R&D on Science and Technology (FIRST), Japan.

[1] E. Bauer, G. Hilscher, H. Michor, C. Paul, E. W. Scheidt, A. Gribanov, Yu. Seropegin, H. Noël, M. Sigrist, and P. Rogl, Phys. Rev. Lett. **92**, 027003 (2004).
[2] K. Togano, P. Badica, Y. Nakamori, S. Orimo, H. Takeya, and K. Hirata, Phys. Rev. Lett. **93**, 247004 (2004).
[3] H. Q. Yuan, D. F. Agterberg, N. Hayashi, P. Badica, D. Vandervelde, K. Togano, M. Sigrist, and M. B. Salamon, Phys. Rev. Lett. **97**, 017006 (2006).
[4] N. Kimura, K. Ito, K. Saitoh, Y. Umeda, H. Aoki, and T. Terashima, Phys. Rev. Lett. **95**, 247004 (2005).
[5] A. D. Hillier, J. Quintanilla, and R. Cywinski, Phys. Rev. Lett. **102**, 117007 (2009).
[6] L. P. Gorkov and E. I. Rashba, Phys. Rev. Lett. **87**, 037004 (2001).
[7] Y. Kamihara, T. Watanabe, M. Hirano, and H. Hosono, J. Am. Chem. Soc. **130**, 3296 (2008).
[8] H. Barz, H. C. Ku, G. P. Meisner, Z. Fisk, and B. T. Matthias, Proc. Natl. Acad. Sci. USA. **77**, 3132 (1982).
[9] I. Shirotani, Bull. Chem. Soc. Jpn. **76**, 1291 (2003).
[10] TOPAS 2005 Version 3(Karlsruhe, Germany: Bruker AXS).
[11] G. Kresse and J. Furthmüller, Phys. Rev. B **54**, 11169 (1996).
[12] J. P. Perdew, K. Burke, and M. Ernzerhof, Phys. Rev. Lett. **77**, 3865 (1996).
[13] O. L. Sologub, P. S. Salamakha, T. Sasakawa, X. Chen, S. Yamanaka, and T. Takabatake, J. Alloys Compd. **345**, 6 (2002).
[14] A. Loehken, G. J. Reiss, D. Johrendt, and A. Mewis, Z. Anorg. Allg. Chem. **631**, 1144 (2005).
[15] K. Klepp and E. Parthe, Acta Cryst. B **38**, 1105 (1982).
[16] A. H. Wilson, Proc. R. Soc. Lond. A **167**, 580 (1938).
[17] F. Kneidinger, H. Michor, A. Sidorenko, E. Bauer, I. Zeiringer, P. Rogl, C. Blaas-Schenner, D. Reith, and R. Podloucky, Phys. Rev. B **88**, 104508 (2013).
[18] S. Ramakrishnan, K. Ghosh, A. D. Chinchure, V. R. Marathe, and G. Chandra, Phys. Rev. B **52**, 6784 (1995).
[19] H. Wiesmann, M. Gurvitch, H. Lutz, A. K. Ghosh, B. Schwarz, M. Strongin, P. B. Allen, and J. W. Halley, Phys. Rev. Lett. **38**, 782 (1977).
[20] T. Klimczuk, Q. Xu, E. Morosan, J. D. Thompson, H. W. Zandbergen, and R. J. Cava, Phys. Rev. B **74**, 220502 (2006).
[21] E. Bauer, R. T. Khan, H. Michor, E. Royanian, A. Grytsiv, N. Melnychenko-Koblyuk, P. Rogl, D. Reith, R. Podloucky, E. W. Scheidt, W. Wolf, and M. Marsman, Phys. Rev. B **80**, 064504 (2009).
[22] L. Fang, H. Yang, X. Zhu, G. Mu, Z. S. Wang, L. Shan, C. Ren, and H. H. Wen, Phys. Rev. B **79**, 144509 (2009).
[23] N. R. Werthamer, E. Helfand, and P. C. Hohemberg, Phys. Rev. **147**, 295 (1966).
[24] A. M. Clogston, Phys. Rev. Lett. **9**, 266 (1962).
[25] J. Bardeen, L. N. Cooper, and J. R. Schrieffer, Phys. Rev. **108**, 1175 (1957).
[26] F. Bouquet, Y. Wang, R. A. Fisher, D. G. Hinks, J. D. Jorgensen, A. Junod, and N. E. Phillips, EPL **56**, 856 (2001).
[27] H. Okamoto, H. Taniguti, and Y. Ishihara, Phys. Rev. B **53**, 384 (1996).
[28] See Supplemental Material at http://link.aps.org/supplemental/10.1103/PhysRevB.89.024517 for XRD patterns of LaMPn (M = Ir and Rh; Pn = P and As), Temperature dependence of resistivity measured at various magnetic fields for LaIrAs and LaRhP and Electronic band structures of LaIrAs, LaRhP and LaRhAs.
[29] W. L. McMillan, Phys. Rev. **167**, 331 (1968).